BBAA VI International Colloquium on:
Bluff Bodies Aerodynamics & Applications
Milano, Italy, July, 20–24 2008

3D FLOW AROUND A RECTANGULAR CYLINDER: A COMPUTATIONAL STUDY

Arianna Bosco[⋆], **Luca Bruno**[†], **Nicolas Coste**[‡] **and Davide Fransos**[*]

[⋆]Aachen Institut for advanced studies in Computational Engineering Science
RWTH Rheinisch-Westflische Technische Hochschule Aachen, Pauwelstrasse 12, 52074 Aachen, Germany
e-mail: `bosco@aices.rwth-aachen.de`

[†]Dipartimento di Ingegneria Strutturale e Geotecnica
Politecnico di Torino, Viale Mattioli 39, 10126 Torino, Italy
e-mail: `luca.bruno@polito.it`

[‡]OptiFlow Company
Hôtel Technologique B.P. 100, Technopôle de Château Gombert, 13382 Marseille, France
e-mail: `coste@optiflow.fr`

[*] Dipartimento di Matematica
Politecnico di Torino, Corso Duca degli Aruzzi 24, 10129 Torino, Italy
e-mail: `davide.fransos@polito.it`

Keywords: Computational Wind Engineering, Large Eddy Simulation, rectangular cylinder

1 INTRODUCTION

The aim of this paper is to provide a contribution to the study of the 3D, high Reynolds number, turbulent, separated and reattached flow around a fixed rectangular cylinder with chord-to-depth ratio equal to 5. In spite of the simple geometry, it is believed that the problem is of interest not only for the purpose of fundamental research, but also to provide useful information on the aerodynamics of a wide range of bluff bodies of interest in Civil Engineering (e.g. long span bridges decks, high-rise buildings, and so on) and in other Engineering applications.

A number of studies have been devoted to the aerodynamic behaviour of this bluff body since the reference experimental works of Okajima [1] and Norberg [2]. On one hand, the low-Reynolds number flow around rectangular cylinders has been clarified in both its 2D and 3D features by several studies (e.g. [3, 4, 5]. On the other hand, the high-Reynolds number flow (i.e. $Re \geq 1.e + 4$) has been studied by means of both experimental and computational approach, with emphasis on both its dependence to chord-to-depth ratio [6, 7, 8] and its spanwise coherence pressure characteristics [9]. Neverthless, according to the authors, some difficulties remain in describing the complex flow phenomena that drive the fluctuating aerodynamic forces acting on such kind of cylinders.

The mechanisms responsible for the variation of the fluctuating aerodynamic forces and the 3D features of the flow are scrutinized in this study. The computational approach postprocessing facilities are emploied to look for relevant relationships between flow structures, pressure field and aerodynamic forces.

2 FLOW MODELLING AND COMPUTATIONAL APPROACH

The 3D, turbulent, unsteady flow around the cylinder is modeled in the frame of the Large Eddy Simulation approach to turbulence by the classical time-dependent filtered Navier-Stokes equations, closed by a transport equation for the the kinetic energy k of the unresolved stresses [10]. Dirichlet conditions on the velocity field and on the subgrid kinetic energy are imposed at the inlet boundaries. Neumann conditions involving the velocity field and the pressure (null normal component of the stress tensor) as well as the same Dirichlet conditions on k are imposed at the outlet boundaries. Periodic conditions are imposed on the side surface of the computational domain. No-slip conditions are imposed at the section surface. Impulsive initial conditions are introduced.

The Finite Volume open source code OpenFoam is used in the following to numerically evaluate the flowfield. An unstructured mesh of polyhedral cells is employed. The cell-center values of the variables are interpolated at face locations using a second order Central Difference Scheme for the diffusive terms and Limited Linear scheme for the convection terms [11]. Advancement in time is accomplished by the second-order implicit Euler scheme. The computational grid in space consists of about $6.33e + 6$ cells. The nondimensional timestep needed for an accurate advancement in time is $\Delta t = 1e - 3$. Each simulation is extended along 150 time units in order to overcome the transient solution and to allow the statistic analysis of the periodic flow. Computations are carried out on 8 Intel Quadcore X5355 2.66GHz CPU and require about 2.5GB of memory and 15 days of CPU time for the whole simulation.

3 APPLICATION AND RESULTS

The incoming flow is characterized by the Reynolds number $Re = UD/\nu = 4.0e+4$, where U is the incoming flow velocity, D the deck dept and ν the kinematic viscosity, incidence $\alpha = 0$ and turbulence intensity $It = 1\%$. The cylinder rectangular cross section is characterized by a chord-to-depth ratio $B/D = 5$ and by sharp corners. The spanwise length of the cylinder is equal to $L/D = 5$.

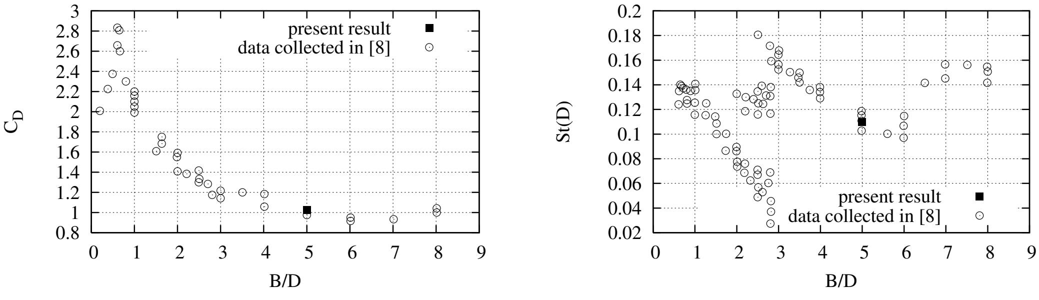

(a) (b)

Figure 1: Mean drag coefficient and Strouhal number: comparison with results in literature

Figure 1 compares the present results with experimental and computational data collected in

[8]. The obtained mean drag coefficient $\overline{C_D}$ and Strouhal number $St = nD/U$, where n is the dominant frequency in the lift spectrum, are in good agreement with the other data obtained at the same chord-to-depth ratio.

Figure 2 gives an example of the attempt in relating the fluctuating lift coefficient $\overline{C_L}(t)$ to the instantaneous flow field, described by pressure distributions and vorticity magnitude isocontours on the central section. It is worth to point out that $(+)$ sign corresponds to counterclockwise eddies, while $(-)$ sign refers to clockwise ones. The low-pressure peaks on the sidesurfaces clearly correspond to the travelling leading-edge vortices. The suction effects of the pairs of leading-edge vortices along the upper and lower side surfaces approximately cancel each other, while the C_L maximum value is mainly due to the high-pressure region close to the lower surface trailing-edge.

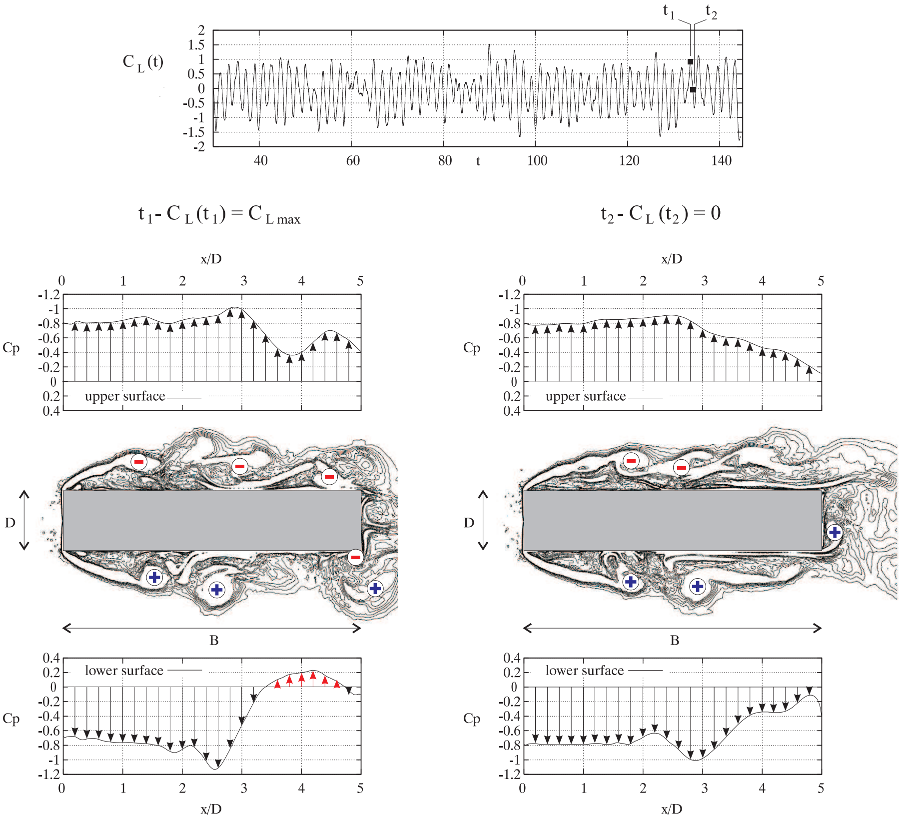

Figure 2: Lift time history, instantaneous Cp distributions and vorticity magnitude isocontours at the central cross section

The 3D features of the flow around the 2D cylinder, mainly located downwind the reattachment point, are qualitativelly shown if Figure 3. The final paper will contain a quantitative description of the 3D flow features by means of coherence function and Proper Ortogonal Decomposition of the side-surface pressure field.

REFERENCES

[1] A. Okajima. Strouhal numbers of rectangular cylinders. *Journal of Fluid Mechanics*, **123**, 379–398, 1982.

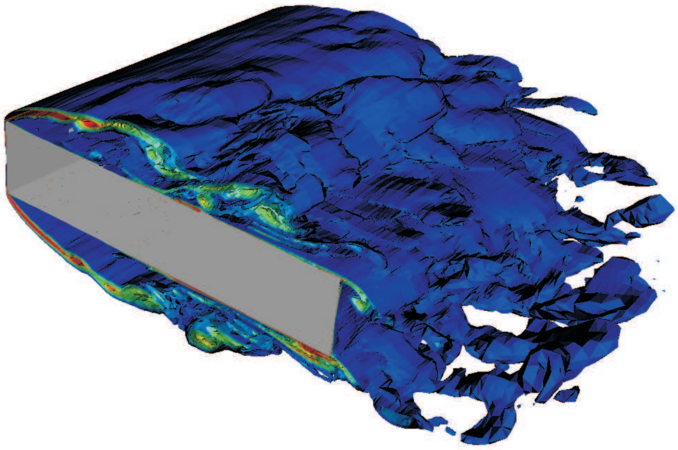

Figure 3: 3D vorticity magnitude isosurface (ω=20)

[2] C. Norberg. Flow around rectangular cylinders: pressure forces and wake frequencies, *Journal of Wind Engineering and Industrial Aerodynamics*, **49**, 187–196, 1993.

[3] Y. Nakamura, Y. Ohya, S. Ozono, R. Nakamaya, Experimental and numerical analysis of vortex shedding from elongated rectangular cylinders at low Reynolds numbers 200-1000. *Journal of Wind Engineering and Industrial Aerodynamics*, **65**, 301–308, 1996.

[4] K. Hourigan, M. C. Thompson, B. T. Tan. Self-sustained oscillations in flows around long blunt plates. *Journal Fluid and Structures*, **15**, 387–398, 2001.

[5] B. T. Tan, M.C. Thompson, F. Hourigan. Flow past rectangular cylinders: receptivity to transverse forcing. *Journal of Fluid Mechanics*, **515**, 33–62, 2004.

[6] D.Yu, A.Kareem. Two-dimensional simulation of flow around rectangular prism. *Journal of Wind Engineering and Industrial Aerodynamics*, **62**, 131–161, 1996.

[7] D.Yu, A.Kareem. Parametric study of flow around rectangular prisms using LES. *Journal of Wind Engineering and Industrial Aerodynamics*, **77-78**, 653–662, 1998.

[8] K. Shimada, T. Ishihara. Application of a modified k-ϵ model to the prediction of aerodynamic characteristics of rectangular cross-section cylinders. *Journal of Fluid and Structures*, **16**, 465–485, 2002.

[9] M. Matsumoto, H. Shirato, K. Aaraki, T. Haramura, T. Hashimoto. Spanwise coherence characreristic of surface pressure field on 2D bluf bodies. *Journal of Wind Engineering and Industrial Aerodynamics*, **91**, 155–163, 2003.

[10] A.Yoshizawa. Statistical theory for compressible shear flows with the application of subgrid modelling. *Physics of Fluids A*, **29**, 2152–2163, 1986.

[11] H.Jasak, H.G.Weller, A.D.Gosman. High resolution NVD differencing scheme for arbitrarily unstructured meshes. *International journal for numerical methods in fluids*, **31**, 431–449, 1999.